analytical chemistry

Letter

Cite This: Anal. Chem. 2018, 90, 7795−7799

pubs.acs.org/ac

Ultrasensitive Plasmonic Biosensors for Real-Time Parallel Detection of Alpha-L-Fucosidase and Cardiac-Troponin-I in Whole Human Blood

Xu Han,[*,†,∥] Hossein Shokri Kojori,[‡,∥] Roger M. Leblanc,[§] and Sung Jin Kim[*,‡]

[†]Huston Labs, 1951 NW Seventh Avenue, Suite 600, Miami, Florida 33136, United States

[‡]Department of Electrical and Computer Engineering, University of Miami, Coral Gables, Florida 33146, United States

[§]Department of Chemistry, University of Miami, Coral Gables, Florida 33146, United States

Supporting Information

ABSTRACT: Cancers and many other diseases, such as hepatocellular carcinoma (HCC) and cardiovascular diseases (CVD), have threatened human lives for centuries. Therefore, a novel technique for such disease prediction is in an urgent demand for timely treatment. Biomarkers, alpha-L-fucosidase (AFU) for HCC and cardiac troponin I (cTnI) for CVD, have proven to be essential in the role of disease detection. Herein, we report on an ultrasensitive plasmonic biosensor that converts plasmonic absorption to electrical current in order to detect AFU and cTnI using whole human blood in a real-time and parallel fashion. The detection limit was calculated to be 0.016 U/L for AFU and 0.015 ng/mL for cTnI, respectively. Combined with the versatility of the strategies for different biomarkers, these results demonstrate that the developed biosensor exhibits a promising application for the prediction of cancers and many other diseases.

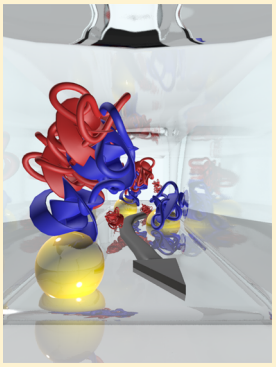

Natural assembly provides a substantial methodology to direct simple building blocks into establishing hierarchical architectures.[1] Certain functions operated by these delicate nanostructures in responds to the incoming stimulation achieve the sophisticated "nano-machines". Seen in photosynthesis, the plant or organism converts the incoming optical energy into a signal which can be effectively captured to perform subsequent and particular actions. The specific and effective transduction occurring in this type of process represents the precise operation in the nature. It is a major goal of biotechnology and nanotechnology to transfer these concepts utilized in the nature into benchtop scientific and engineering technology. As a result, tremendous efforts and progress have gone into antibody−antigen−antibody sandwiched nanostructures.[2] The activities associated with this mode of signal transduction include a three-layer assembly, whereby (a) the first layer (antibody) captures the second layer (antigen), (b) the third "antenna" layer (functionalized antibody) can demonstrate certain measurable properties after attaching to the second layer. Depending on the character of the "antenna", the biomimicking nanostructures are classified into colorimetric,[3] fluorescence,[4] paramagnetic,[5] and electrochemical assay.[6] These indirect signal transduction systems will enable the development of integrated circuits with innovative functions that extend conventional digital components into biosensing areas.

One application of this sandwiched nanostructure is disease prediction by analyzing biomarkers for disease prediction.[7] The secret behind the function of disease prediction involves the fact that life forms are known to shed certain unique biomarkers (antigens) into the bloodstream as evidence of particular biological conditions.[8] Conventional techniques, including electrocardiography (ECG), magnetic resonance imaging (MRI), and computerized tomography (CT) scan, are costly and need relatively complicated analysis. Worse, they are only successful when the tumor grows into a larger size.[9] Inspired by nature, antibody−antigen−antibody based biomarker immunoassay starts to be implemented for detection of several diseases to expedite clinical treatment. While the format of detection strategies varies, a common feature is the implementation of immunoglobulin (IgG). This component allows the immunoassay to be an ideal platform toward the specific detection development. However, the primary limiting factors in these types of detection approaches include the concern of complicated platforms with relatively low sensitivity, long detection time, and poor function with whole human blood samples.[10,11] Major problems as a result of these limitations include (1) indirect detection of stimulated signals, (2) partially quenched signal transduction as a result of the sensing environment, (3) less labeled antibody immobilization due to two times the binding activity, causing a weaker signal intensity. Nowadays, the trend toward point of care diagnostics based on the biomarker detection, by any means, has had a significant impact on the development with which

Received: April 23, 2018
Accepted: June 15, 2018
Published: June 15, 2018

DOI: 10.1021/acs.analchem.8b01816
Anal. Chem. 2018, 90, 7795−7799

potential diagnostic measurements can be designed.[12] The point of care testing (POCT) mainly refers to the medical diagnostic testing in proximity to the patient's location without sending the specimen away from the point of care. To address improvements toward the diagnosis of cancers and many other diseases, it is, hence, urgent that a novel transducer technique be developed with the capability to effectively capture and deliver the information upon biomarker attachment onto the immunoassay in a simple and more accurate fashion.

One such system has arisen with the exploitation of localized surface plasmon resonances (LSPR),[13−15] wherein hot electrons oscillate inside metal nanoparticles in response to light propagation at visible and near-infrared frequencies.[16−18] Conventional LSPR based sensing uses colorimetry based systems that require bulky optical instrumentation. This approach has a limitation in minimizing the size of the sensor system and lowering detection limit by decreasing sensor area. Therefore, a simple device that has the capability to integrate all of the advantages of highly sensitive LSPR based detection, while lowering detection limit is essential for the evolution of POCT technology. To this end, our previous work shows a plasmon-field-effect based thin film transistor with a highly efficient detection of this plasmon energy without the need for bulky optics and instrumentation.[19] This new transducer device offers direct plasmon-to-electric signal conversion and amplification of the detected signal. We also demonstrated superior protein detection capability using this new sensing platform.[20] The gold nanoparticles (AuNPs) utilized in the device displayed a strong plasmonic absorption at visible wavelengths. The plasmonic energy is able to subsequently couple with AuNPs and decay into hot electrons. The gate bias incorporated in the device promotes a successful migration of induced hot electrons to inject over the Schottky barrier. This process exhibits an effective hot electron trapping capability, which operates in a similar way to natural photosynthesis described above. Inspired by nature and motivated in advancements toward significant progress on POCT development, we designed an innovative signal transducer technique, comprised of metal−semiconductor-metal (MSM) structure without an extra gate bias. In the absence of the gate bias, only the voltage at one wavelength is monitored without supply voltage rather than the plasmonic energy from the full spectral response. Our plasmonic sensing platform with special nanostructures uses a wide-bandgap semiconducting material, InGaZnO (IGZO), which is transparent in the visible to infrared spectrum. As a result, the plasmonic nanostructure can be excited from the back side of the platform, leading to a direct detection of the plasmonic energy. This function can resolve the issue of employing colored medium that usually overlaps with light source wavelength. Conventional surface plasmon resonance system with an Au film surface utilizes similar excitation structures. However, our system benefits from a much smaller sensing surface area that allows excellent minimum detection limits. The small active sensing area also requires only a tiny amount of analyte and implements a high integration capability with a multiplexing function. In addition, LSPR platform harbors a better thermal capability without the need for other temperature controls compared to SPR system. To obtain a strong signal-to-noise ratio, lock-in amplification techniques are integrated to enable the system to detect the potentially small photocurrents generated by the short-lived hot electrons. This lock-in amplification approach takes the response signal only from the specific modulation frequency by the excitation light and eliminates other noises from the ionic strength in the medium, pH change, to temperature fluctuations.

To demonstrate the plasmonic sensor operation, two specific biomarkers were selected: (1) alpha-L-fucosidase (AFU), a valuable diagnostic biomarker for hepatocellular carcinoma (HCC),[21] and (2) cardiac troponin I (cTnI), a blood borne biomarker associated with cardiovascular diseases (CVD).[9] It is claimed that HCC, the primary malignancy of liver cancer, remains one of the most commen and deadly cancers worldwide,[21] while CVD is considered to be the leading global cause of death, accounting for 17.3 million mortalities annually.[9] The concentration of AFU and cTnI to separate the healthy people from the afflicted patients were suggested to be 50 U/L[22] and 0.5 to 2.0 ng/mL,[9] respectively. It is not a facile task to develop AFU or cTnI biosensors, especially with the AFU. AFU is characterized as a lysosomal enzyme, enabling hydrolytic cleavage of fucose-containing molecules. Therefore, most research has been focused on the immunoassay that utilizes this enzymatic property, resulting in much more difficult laboratory procedures and works up. In spite of more sensing options available for detecting cTnI, both cTnI and AFU detection systems tend to require diagnostic detectors that involve bulky systems that have low potential for POCT translation.

Initially, the plasmon biosensor was fabricated on a silica substrate with a thin n-type IGZO film. A metal−semiconductor−metal photoconductor was created after two electrodes were separately anchored by depositing Cr/Au layers. Thereafter, AuNPs thereafter were incorporated onto the IGZO thin film between two electrodes (Figure 1a), aiming to deliver a photo response from the plasmonic absorption on the photoconductor. The as-prepared devices were initially characterized using a custom electro-optical measurement setup (Figure S5), whereby a source meter was applied to measure the electrical properties and have the device be biased with dc voltage. The plasmonic spectral response was regulated by a modulated monochromatic light with a lock-in amplifier. A customized LabView program was employed to control the monochromator, a lock-in amplifier, and a picoammeter, to obtain an automated computerized measurement. Based on the preliminary characterization of the sensing unit, we identified the best conditions for voltage bias and the wavelength for optical response (Figure S4). The current generated from the plasmonic induced hot electrons passed through a 100 kΩ resistor as shown in Figure S5, providing a signal of plasmonic sensor with a voltage unit. Finally, the sensing platform was placed in a 3D printed housing accompanied by a green light emitting device (LED) at the bottom. A narrow bandwidth optical filter was utilized to build a miniaturized sensor package as shown in Figure S7. The monochromatic light was delivered through the glass substrate from the bottom of the sensor. This configuration carries out a direct illumination of LED light to the plasmonic AuNPs, avoiding light absorption by blood or other medium. More details with regard to the device fabrication are available in the Supporting Information.

To minimize the sample size and further achieve multiplexing detection of both AFU and cTnI or other multibiomarkers, a poly(dimethylsiloxane) (PDMS) based microfluidic channel was prepared by polymer casting. More details about the construction of microfluidic channel are described in the Supporting Information. The as-prepared microfluidics,

DOI: 10.1021/acs.analchem.8b01816
Anal. Chem. 2018, 90, 7795−7799

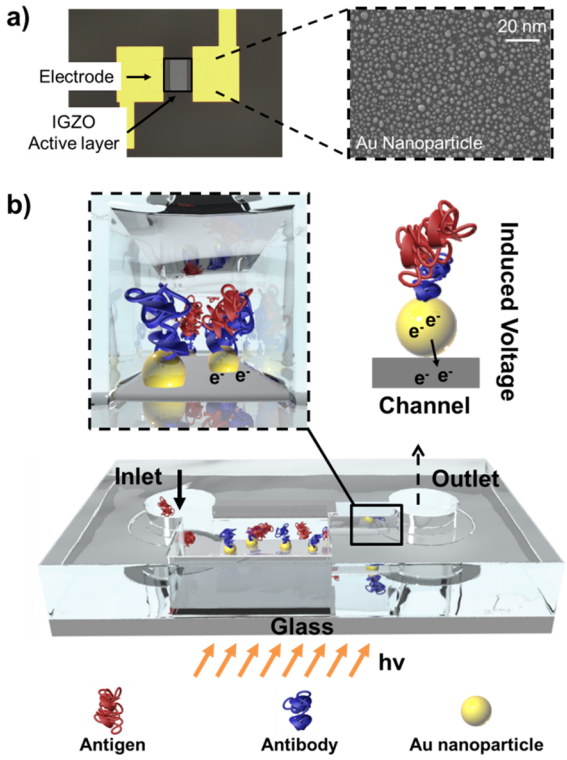

Figure 1. (a) Chip design of the biosensor with AuNPs immobilized on the surface of the IGZO active layer between two gold electrodes. The inset shows the SEM image of AuNPs. (b) Cross-section of the parallel flow through biosensor with microfluidic channel. Inset displays the induced electron flow from the AuNP when antigen is bound to antibody.

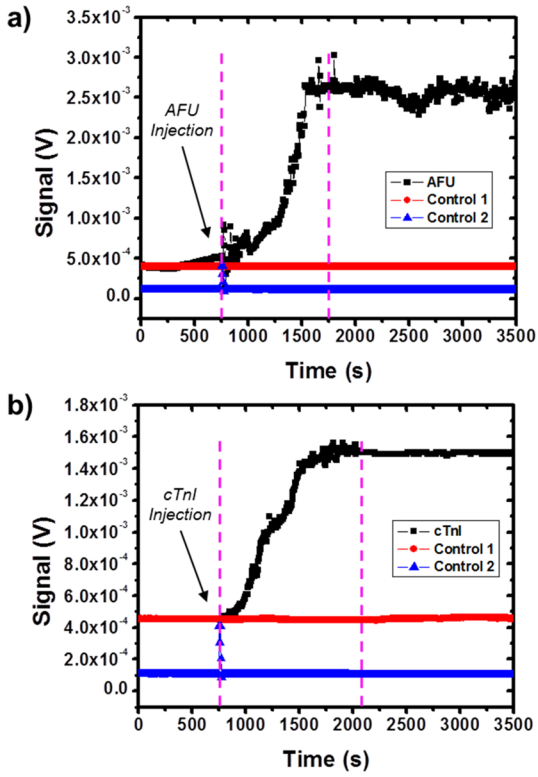

Figure 2. Real-time measurement of (a) AFU and (b) cTnI detection with blind protein control (red line) and gold nanoparticle control (blue line). The mixed PBS buffer solutions with 4 U/L AFU and 0.1 ng/mL cTnI were injected into the biosensor at 750 s, respectively. The signal was stabilized at around 1750 s.

where four independent microchannels were present, were carefully aligned onto the biosensor under optical microscopy in order to keep the sample parallel across the sensing platform. Next, 1 mM 3-mercaptopropionic acid (MPA) ethanoic solution was injected into the microfluidic channel so as to modify the AuNPs. This allows the biomarker antibody to conjugate onto the AuNPs via 1-ethyl-3-(3-(dimethylamino)propyl) carbodiimide hydrochloride (EDC) and *N*-hydroxysuccinimide (NHS) chemistry. The large surface to volume ratio associated with AuNPs provides a distinct advantage for higher loading capacity. After approximately 1 h incubation, 1% bovine serum albumin (BSA) was added to block the nonspecific binding sites.

First, AFU and cTnI detection were performed by separately injecting 2 μL samples in PBS buffer (pH = 7.4) with the sensor being turned on in advance. Figure 2 illustrates the real-time measurement where the current fluctuates upon the injection of the sample, in particular for the AFU case. This fluctuation is attributed to the collision of the antigen against the modified AuNPs, digitally representing the binding process during antibody−antigen interactions. The reason behind it is that the environment surrounding the nanostructure has an impact on the hot electron generated from the plasmonic absorption, thereby causing the correlation of voltage signal to the "effective refractive index" surrounding AuNPs. The voltage, indicative of antigen absorbance intensity, was recorded as a function of time. It remained stable in approximately 1000 s after sample injection, suggesting the completion of the antibody−antigen binding activity (Figure 2). To study the device-to-device variation, three of each biosensor were exposed in tandem to five different concentrations of AFU and cTnI, respectively. The as-prepared biosensors have a maximum standard deviation of 12.47% for AFU and 2.49% for cTnI. By plotting the signal against different AFU and cTnI concentrations, LOD was calculated to be 0.016 U/L and 0.015 ng/mL, respectively (Figure 3). Both

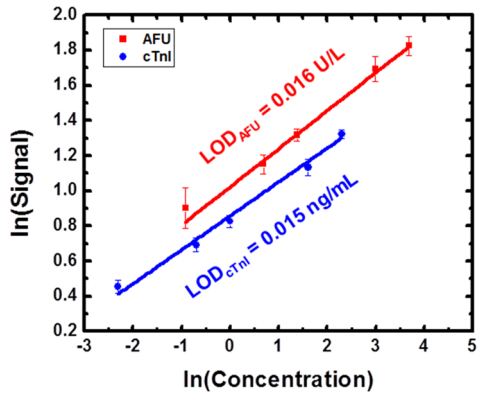

Figure 3. Plot of different concentrations of AFU (red spots) and cTnI (blue spots) against their corresponding signals.

values are much lower than the concentration required to separate the patients from normal people. The calculation was based on the sum of the *y*-intercept from the calibration curve and three times the standard deviation. In comparison to other immunoassays (Table 1), our methodology demonstrates a unique parallel detection of different biomarkers at the same

DOI: 10.1021/acs.analchem.8b01816
Anal. Chem. 2018, 90, 7795−7799

Table 1. Performance and Detection Methods of Different Immunoassays

target	method	analytic time (min)	LOD	POCT potential
cTnI[23]	colorimetric	30	0.1 ng/mL	low
cTnI[24]	paramagnetic	4.1	0.5 ng/mL	medium
cTnI[25]	electrochemical	60	0.2 ng/mL	low
cTnI[26]	SPR	15	1.4 ng/mL	medium
AFU[27]	colorimetric	6	0.01 U/L	medium
AFU[28]	spectrofluorometric	>30	46 U/L	medium
AFU[29]	spectrofluorometric		0.28 U/L	medium
AFU[30]	electrophoresis		46 U/L	medium

time. In addition, most previous studies have detected AFU by analyzing the absorbance of yellow colored species produced in the AFU catalytic reaction. This approach suffered from interference from the colored serum of patient samples. Our methodology, instead, can generate the analyte signal when the biomarker was captured on the detection platform. This further promotes this technique for the future development of POCT diagnostics.

To further confirm this proof of concept, a series of control experiments were examined, including measurement without the presence of AuNPs and blind protein detection. AuNPs are the key to the whole detection mechanism. The absence of the AuNPs, or the physiological absorption of AFU or cTnI to the detection platform surface, thus, presents negligible results with regard to the detection of the different biomarkers. This hypothesis is consistent with the observation in Figure 2, where the same procedures were followed as described above in the absence of AuNPs. Other than AFU and cTnI, insulin was also injected into the device as a blind protein sensing test. As expected, negligible results were observed in the detection window due to poor binding of nonspecific secondary antibody to insulin, strongly indicating the specificity of the constructed biosensor.

It is well-known that proteins adopt different conformations in different environments, resulting in an impact on the antibody−antigen interactions. Whole human blood has one of the most complex matrixes filled with ample substrates that can create false readings. The complexity of working in whole human blood is a dominant scientific challenge in detection technology, particularly for the optical sensing technology due to the absorption from the blood. To develop a device that can be applied to whole human blood would show great achievement in the field. As a proof-of-concept, whole human blood was selected for investigation on the AFU and cTnI detection. 0.2 U/L AFU and 0.1 ng/mL cTnI were mixed with whole human blood, respectively. Sample injections where the biomarker was added proceeds faster (kinetic) than samples where the biomarker was not added. This should be attribute to the additional interaction of the biomarker to the antibody attached on the surface, in addition to other nonspecific interactions occurring at the interface. By comparing the control experiment (whole human blood without any biomarkers), Figure 4 demonstrates a similar curve, the sensing signals are over 12% in contrast to the pure whole human blood control results, to previous tests in detection measurements, thus confirming that this portable plasmonic biosensor has a great potential for clinical analysis.

In conclusion, the portable plasmonic biosensor was fabricated by incorporating microfluidic channels on a

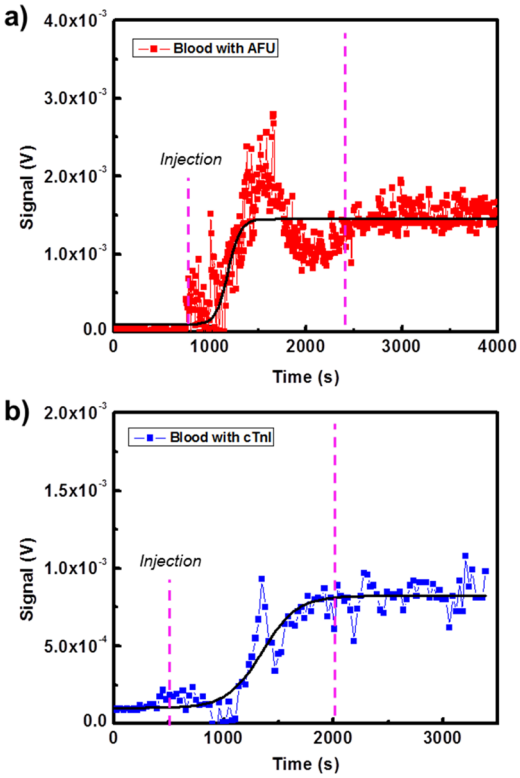

Figure 4. Real-time measurement of detecting (a) 0.2 U/L AFU and (b) 0.1 ng/mL cTnI mixed with whole human blood, respectively, and the control experiments with the pure whole human blood (red spots).

designed microchip. The AuNPs embedded into the channel of the microchip were conjugated with specific antibodies to enable the specificity of the whole system. Furthermore, the developed biosensor has a significant potential for POCT as well as the capability for real time dynamic interaction monitoring of different biomarkers in a tandem and parallel fashion. Considering the high sensitivity toward AFU and cTnI, where the LOD is calculated to be 0.016 U/L and 0.015 ng/mL, respectively, and the wide applicable strategies for other biomarkers along with the excellent platform for whole human blood samples, this plasmonic biosensor can help lead to breakthroughs in the sensing nanotechnology and future clinical use.

■ ASSOCIATED CONTENT

Supporting Information

The Supporting Information is available free of charge on the ACS Publications website at DOI: 10.1021/acs.analchem.8b01816.

General methods, plasmon biosensor fabrication, microfluidic channel fabrication, electro optical characterization, and sensor packaging and measurement (PDF)

■ AUTHOR INFORMATION

Corresponding Authors

*E-mail: x.han5@umiami.edu.
*E-mail: kim@miami.edu.

ORCID

Xu Han: 0000-0001-9095-1755
Roger M. Leblanc: 0000-0001-8836-8042

DOI: 10.1021/acs.analchem.8b01816
Anal. Chem. 2018, 90, 7795−7799

Author Contributions

[‖]X.H. and H.S.K. contributed equally. H.S.K. fabricated the device. X.H. functionalized the device. X.H. and H.S.K. analyzed the data. X.H. wrote the manuscript with revisions from H.S.K. and S.J.K. S.J.K. supervised the project.

Notes

The authors declare no competing financial interest.

■ ACKNOWLEDGMENTS

X.H. acknowledges the support from the University of Miami and Huston Labs. X.H. especially acknowledges the support from Tom Huston, Jr., Catherine H. Lorié, and Edward D. Miller. X.H. and R.M.L. gratefully acknowledge the financial support from National Science Foundation (Grant 1355317). X.H. appreciates revisions from Catherine J. Munro. R.M.L. gratefully acknowledges the financial support from King Abdulaziz University. S.J.K acknowledges the financial support by John T. MacDonald Foundation and the National Science Foundation (Grant CBET-1605325).

■ REFERENCES

(1) Han, X.; Zheng, Y.; Munro, C. J.; Ji, Y.; Braunschweig, A. B. *Curr. Opin. Biotechnol.* **2015**, *34*, 41−47.
(2) Shen, J.; Li, Y.; Gu, H.; Xia, F.; Zuo, X. *Chem. Rev.* **2014**, *114*, 7631−7677.
(3) Liu, J.; Lu, Y. *Angew. Chem., Int. Ed.* **2006**, *45*, 90−94.
(4) Wu, J.; Liu, W.; Ge, J.; Zhang, H.; Wang, P. *Chem. Soc. Rev.* **2011**, *40*, 3483−3495.
(5) Liu, J.; Lu, Y. *J. Am. Chem. Soc.* **2007**, *129*, 9838−9839.
(6) Zuo, X.; Xiao, Y.; Plaxco, K. W. *J. Am. Chem. Soc.* **2009**, *131*, 6944−6945.
(7) Sawyers, C. L. *Nature* **2008**, *452*, 548−552.
(8) Strimbu, K.; Tavel, J. A. *Curr. Opin. HIV AIDS* **2010**, *5*, 463−466.
(9) Han, X.; Li, S.; Peng, Z.; Othman, A. M.; Leblanc, R. *ACS Sens.* **2016**, *1*, 106−114.
(10) Gaster, R. S.; Hall, D. A.; Nielsen, C. H.; Osterfeld, S. J.; Yu, H.; Mach, K. E.; Wilson, R. J.; Murmann, B.; Liao, J. C.; Gambhir, S. S.; Wang, S. X. *Nat. Med.* **2009**, *15*, 1327−1332.
(11) Arlett, J. L.; Myers, E. B.; Roukes, M. L. *Nat. Nanotechnol.* **2011**, *6*, 203−215.
(12) Tudos, A. J.; Besselink, G. J.; Schasfoort, R. B. *Lab Chip* **2001**, *1*, 83−95.
(13) Mayer, K. M.; Hafner, J. H. *Chem. Rev.* **2011**, *111*, 3828−3857.
(14) Anker, J. N.; Hall, W. P.; Lyandres, O.; Shah, N. C.; Zhao, J.; Van Duyne, R. P. *Nat. Mater.* **2008**, *7*, 442−453.
(15) Willets, K. A.; Van Duyne, R. P. *Annu. Rev. Phys. Chem.* **2007**, *58*, 267−297.
(16) Atwater, H. A.; Polman, A. *Nat. Mater.* **2010**, *9*, 205−213.
(17) Knight, M. W.; Sobhani, H.; Nordlander, P.; Halas, N. J. *Science* **2011**, *332*, 702−704.
(18) Okamoto, K.; Niki, I.; Shvartser, A.; Narukawa, Y.; Mukai, T.; Scherer, A. *Nat. Mater.* **2004**, *3*, 601−605.
(19) Shokri Kojori, H.; Yun, J. H.; Paik, Y.; Kim, J.; Anderson, W. A.; Kim, S. J. *Nano Lett.* **2016**, *16*, 250−254.
(20) Kojori, H. S.; Ji, Y.; Paik, Y.; Braunschweig, A. B.; Kim, S. J. *Nanoscale* **2016**, *8*, 17357−17364.
(21) Malaguarnera, G.; Giordano, M.; Paladina, I.; Berretta, M.; Cappellani, A.; Malaguarnera, M. *Dig. Dis. Sci.* **2010**, *55*, 2744−2755.
(22) Zhang, S. Y.; Lin, B. D.; Li, B. R. *FEBS Open Bio* **2015**, *5*, 240−244.
(23) Liu, J.; Zhang, L.; Wang, Y.; Zheng, Y.; Sun, S. *Measurement* **2014**, *47*, 200−206.
(24) Kiely, J.; Hawkins, P.; Wraith, P.; Luxton, R. *IET Sci., Meas. Technol.* **2007**, *1*, 270−275.
(25) Bhalla, V.; Carrara, S.; Sharma, P.; Nangia, Y.; Suri, C. R. *Sens. Actuators, B* **2012**, *161*, 761−768.
(26) Masson, J.-F.; Obando, L.; Beaudoin, S.; Booksh, K. *Talanta* **2004**, *62*, 865−870.
(27) Chen, Z.; Ren, X.; Meng, X.; Zhang, Y.; Chen, D.; Tang, F. *Anal. Chem.* **2012**, *84*, 4077−4082.
(28) El-Shahawi, M. S.; Othman, A. M.; El-Houseini, M. E.; Nashed, B.; Elsofy, M. S. *Talanta* **2009**, *80*, 19−23.
(29) Attia, M. S.; Othman, A. M.; Abualy, M. M.; Abdel-Mottaleb, M. S. *Anal. Chem.* **2010**, *82*, 6230−6236.
(30) Othman, A. M.; El-Houseini, M. E.; El-Sofy, M. S.; Aboul-Enein, H. Y. *Anal. Bioanal. Chem.* **2011**, *400*, 787−795.

DOI: 10.1021/acs.analchem.8b01816
Anal. Chem. 2018, 90, 7795−7799